

PHYSICAL REVIEW LETTERS

VOLUME 71

25 OCTOBER 1993

NUMBER 17

Numerical Chaos, Roundoff Errors, and Homoclinic Manifolds

Mark J. Ablowitz, Constance Schober, and Ben M. Herbst*

Program in Applied Mathematics, University of Colorado, Boulder, Colorado 80309

(Received 22 March 1993)

The focusing nonlinear Schrödinger equation is numerically integrated over moderate to long time intervals. In certain parameter regimes small errors on the order of roundoff grow rapidly and saturate at values comparable to the main wave. Although the constants of motion are nearly preserved, a serious phase instability (chaos) develops in the numerical solutions. The instability is found to be associated with homoclinic structures and the underlying mechanisms apply equally well to many Hamiltonian wave systems.

PACS numbers: 03.40.Kf, 02.60.-x, 02.70.-c, 02.90.+p

In this Letter we discuss extensive moderate to long time numerical experiments which we have carried out on the focusing nonlinear Schrödinger (NLS) equation with periodic boundary conditions. The NLS equation is a well known Hamiltonian nonlinear wave system which arises in many areas of physics, and is special among such problems since a large class of solutions can be computed via the inverse scattering transform (IST) (e.g., [1]); the NLS equation is said to be “integrable.” There are two cases of physical interest—the focusing and defocusing NLS. In the focusing case, when periodic boundary conditions are imposed, the NLS equation has complicated homoclinic structures which under perturbations can produce chaotic dynamics (e.g., [2]). The periodic NLS serves as a useful model describing unstable wave phenomena (e.g., instability in deep water waves) and has been the subject of numerical simulations and laboratory experiments (e.g., [3]).

In our investigations, we employ two numerical schemes which have been used extensively and effectively by researchers studying the NLS equation: (a) the integrable discrete NLS (IDNLS) equation (e.g., [2,4]) and (b) the Fourier split-step (FSS) algorithm (e.g., [5]). The IDNLS equation is an integrable differential-difference equation [4] and is implemented using a high order time discretization. The FSS algorithm, although not integrable, preserves the underlying symplectic structure of the NLS equation and, as such, is in the class of symplectic integrators which have been used as a means of tracking the long time behavior of Hamiltonian systems

(e.g., [6] and references therein). We use two numerical schemes to demonstrate that the results obtained are due to the extreme sensitivity of the periodic focusing NLS equation (in the parameter regime described below) and not the particular details of the numerical schemes employed. To be brief we mainly discuss the calculations of IDNLS. The FSS algorithm yields analogous results.

In earlier work we have shown that initial data which are nearby low dimensional “homoclinic manifolds” trigger numerically induced joint spatial and temporal chaos in nonintegrable numerical schemes at intermediate values of the mesh size [2]. This chaos disappears as the mesh is refined. In this Letter we concentrate on a more troubling aspect of numerically induced chaos. We show that temporal instabilities and chaos can be easily excited by very small perturbations—on the order of roundoff. Although our discussion centers on the NLS equation, we have observed analogous behavior in other problems such as the sine-Gordon and modified Korteweg-de Vries (KdV) equations. We believe that similar results will be found in many other Hamiltonian systems. The NLS equation is an excellent paradigm system to study since we have a great deal of analytical knowledge about this equation, and it is reasonably straightforward to compute.

We begin by summarizing our main observations.

(1) Tiny numerical errors (i.e., 10^{-16}) grow rapidly, eventually saturate, but significantly alter the solution after moderate times. For example, spatially even initial values must evolve in an even manner. However, without

imposing evenness as a separate constraint, we find that an odd component is excited and develops into a size comparable with the “main wave.” Alternatively, calculating in mathematically but not computationally equivalent ways (e.g., simply by reordering terms in the equation) shows that small errors on the order of roundoff grow rapidly and eventually destroy the “true” solution.

(2) In the Hamiltonian framework, the periodic spectrum (see below) provides the “actions” in an action-angle description and they are constants of the motion. We verify that these constants are preserved by the numerical scheme to very high precision.

(3) The sensitivity is due to the proximity to the underlying homoclinic orbits of the NLS equation. It turns out that for the range of initial values we have chosen the splitting distance between suitable complex eigenvalues of the periodic spectrum is extremely small. Such initial data occur naturally and can be associated with the evolution of nearly elementary plane waves as well as waves which evolve into complicated nonlinear states.

(4) After the growth of the small errors, the corresponding state evolves, but not in a quasiperiodic temporal manner as might have been expected based on the integrability of NLS. The power spectrum of the associated evolution has a slowly decaying “tail” whose size grows as the number of linearly unstable modes (i.e., the suitable complex eigenvalues) increases.

(5) Analogous solutions of the defocusing NLS are stable. They are not sensitive, and we have no difficulty in computing the solution over long times, using either IDNLS or FSS. The power spectrum remains compact and, computationally, the solution is quasiperiodic in time. The inverse scattering theory of the focusing NLS equation with periodic boundary values is significantly different from the defocusing NLS or the KdV equation [7]. Defocusing NLS and KdV are analogous to finite dimensional Hamiltonian systems whose underlying geometric structures are compact tori. In these cases, without homoclinic structures, symplectic integrators are effective.

We consider the NLS equation in the form

$$iu_t + u_{xx} + 2s|u|^2u = 0, \quad (1)$$

where $s = \pm 1$ (+1 focusing, -1 defocusing), with periodic boundary conditions $u(x-L/2) = u(x+L/2)$ and initial values $u(x,0) = g(x)$. In the focusing case, the plane wave solution, $u_0(x,t) = a \exp(2i|a|^2t)$, is linearly unstable. When considering small perturbations of the form $u(x,t) = u_0(x,t)[1 + \epsilon(x,t)]$, one can establish that the perturbation is separated into solutions of the form $\epsilon(x,t) \propto \exp(i\mu_n x) \exp(\sigma_n t)$, where $\mu_n = 2\pi n/L$ and the growth rate σ_n is given by $\sigma_n = \mu_n \sqrt{4|a|^2 - \mu_n^2}$. Consequently, the solution is unstable provided $0 < \mu_n^2 < 4|a|^2$. The number of unstable modes is the largest integer M satisfying $0 < M < |a|L/\pi$. The fastest growth rate corresponds to a value $n(\mu_n)$ for which σ_n is maxi-

mal (i.e., closest to $2|a|^2$).

To solve the NLS via IST we use the associated linear scattering problem

$$v_{1x} = -i\lambda v_1 + u(x,t)v_2, \quad (2)$$

$$v_{2x} = i\lambda v_2 - su^*(x,t)v_1, \quad (3)$$

where u^* is the complex conjugate of u and the parameter λ is an eigenvalue once boundary values are specified. The spectrum of this linear operator is invariant under the NLS flow and the periodic or antiperiodic eigenvalues $\{\lambda_i\}_{i=1}^\infty$ provide sufficient invariants to establish the integrability of the NLS. The conserved integrals $\int_{-L/2}^{L/2} T_i \times dx = C_i, i=1,2,\dots$ such as the L^2 norm $T_1 = |u|^2$, the momentum $T_2 = uu_x^*$, and the Hamiltonian $T_3 = |u_x|^2 + |u|^4$ are related to the above eigenvalues.

The IDNLS equation is given by [2,4]

$$iu_{nt} + (u_{n+1} + u_{n-1} - 2u_n)/h^2 + s|u_n|^2(u_{n+1} + u_{n-1}) = 0 \quad (4)$$

with $u_n(t) = u(nh,t)$, $u_{n-N/2}(t) = u_{n+N/2}(t)$, $n=0, 1, \dots, N$ (N even), $h=L/N$, $s = \pm 1$. Since IDNLS is integrable, it possesses the special properties inherent in such systems. As $h \rightarrow 0$ (4) converges to (1) with accuracy $O(h^2)$. In our numerical simulations the time integration of this system of ordinary differential equations is performed by the adaptive Runge-Kutta-Merson routine (D02BBF) in the NAG (numerical algorithms group) software library. We specify an extremely high tolerance to ensure that the results are not dependent upon the time integration. For a description of the FSS algorithm see, for example, [5]. We only remark that in each partial step of the FSS algorithm, the canonical symplectic structure of the NLS equation is preserved, hence the FSS algorithm is a symplectic integrator.

We first discuss our calculations associated with the initial data $g(x,\epsilon) = a(1 + \epsilon \cos \mu x)$, where $a=1.5$, $\mu = 2\pi/L$, $L=4\pi\sqrt{2}$, and $\epsilon=10^{-12}$. From the linear theory discussed above, we see that $g(x,\epsilon)$ contains eight unstable modes. In Fig. 1 we plot the results of IDNLS where we use 512 grid points. In Fig. 1(a) we plot the growth of asymmetry [from (1) note that $g(x,\epsilon)$ is an even function and should have evolved in an even manner]. The asymmetry is measured by $\log_{10}|\hat{f}_6 - \hat{f}_{-6}|$ where \hat{f}_6 is the sixth Fourier harmonic [$u = \sum \hat{f}_m \exp(i\mu_m x)$]. The asymmetry grows exponentially fast; for a while the rate of growth is consistent with that predicted by the maximum growth rate of the linearly unstable plane wave (i.e., $\sigma_{\max} \approx 4.5$). Note that the asymmetry reaches $O(1)$ before it saturates. In Fig. 1(b) an averaged amplitude of the Fourier transform is depicted. Let $\hat{u}_j(k)$ be the Fourier transform of $u_j(t)$ [$u_j(t)$ is evaluated at every $\Delta t=0.2$]; we plot the average: $f_{\text{ave}}(k) = \sum_{j=1}^N |\hat{u}_j(k)|/N$ vs k . We note that the Fourier spectrum has a slowly decaying asymptotic “tail” which is inconsistent with the expectation of a quasiperiodic temporal flow. Note espe-

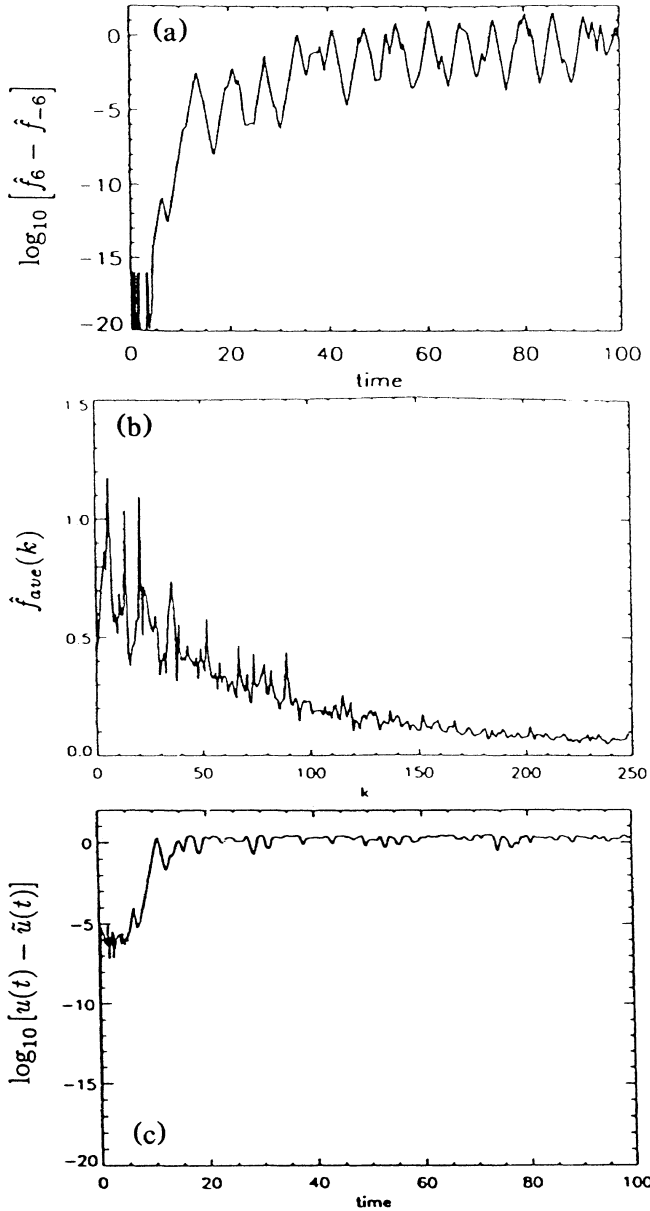


FIG. 1. (a) The asymmetry for IDNLS with $g(x, \epsilon=10^{-12})$. (b) The power spectrum for IDNLS with $g(x, \epsilon=10^{-12})$. (c) The growth in the difference of solutions for IDNLS with $g(x, \epsilon=10^{-12})$.

cially the comparison with the Fourier spectrum of the defocusing NLS equation (Fig. 4). In Fig. 1(c) we plot the logarithm of the averaged difference of two solutions: $\log_{10} \sum_{j=0}^{N/2} |u_j(t) - \tilde{u}_j(t)| / (N+1)$ where $u_j(t)$ is the solution calculated on $(-L/2, L/2)$ and $\tilde{u}_j(t)$ is the solution calculated on $(0, L/2)$ with symmetry imposed, i.e., $u_{-n}(t) = u_n(t)$ (i.e., we calculated on half the lattice). In these calculations the “dominant” complex eigenvalues in the upper half plane were nearly isospectral. The relative change of the first five conserved quantities $\{C_i\}_{i=1}^5$ was

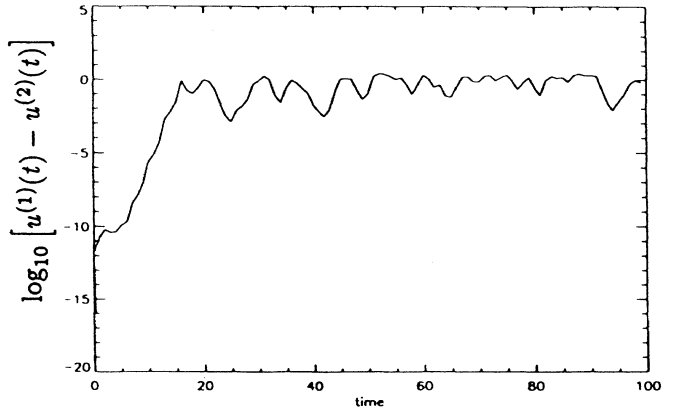


FIG. 2. The growth in the difference of solutions for IDNLS with $g(x, \epsilon=10^{-1})$.

less than 0.01%. As we vary ϵ in $g(x, \epsilon)$ we find similar results; although for significantly larger ϵ (e.g., $\epsilon=10^{-1}$) it takes longer before the asymmetric perturbations “organize” into rapid growth.

As a crude model of roundoff effects we add to the solution [e.g., $g(x, \epsilon)$ with $\epsilon=10^{-1}$] a small random perturbation at each time step: $\epsilon_1 r(x, t)$, where $0 < r < 1$ (r is obtained via a random number generator) for a range of ϵ_1 : $10^{-8}, 10^{-9}, \dots, 10^{-14}$. The main features observed before hold: rapid growth of asymmetry, a slowly decaying tail in the power spectrum, etc.

Even if we impose evenness as a constraint, errors on the order of roundoff grow rapidly. For example, consider IDNLS with the initial values $g(x, \epsilon)$ with $\epsilon=10^{-1}$ and $u_{-n}(t) = u_n(t)$ imposed. We first calculate IDNLS in precisely the way Eq. (4) is specified for $t=0-100$ —call this solution $u_n^{(1)}$. Next we calculate (4) only by distributing the nonlinear terms, i.e., using $s|u_n|^2 u_{n+1} + s|u_n|^2 u_{n-1}$. Call this solution $u_n^{(2)}$. The logarithm of the averaged difference between the solutions, $\sum_{j=0}^{N/2} \log_{10} |u_j^{(1)}(t) - u_j^{(2)}(t)| / (N/2+1)$, grows rapidly (Fig. 2) and, as was the case with asymmetry, the solutions become drastically different. We note that the power spectra of each is broad banded and different from one another as well (not plotted here).

Strongly nonlinear states are unstable and experience the same loss of predictability associated with the above phenomena. For initial data $g(x, \epsilon)$ with $\epsilon=10^{-1}$ we calculate the solution via IDNLS for $t=0-25$. At $t=25$ we are into the fully nonlinear regime and using these values as initial data, we then calculate the two solutions (above): $u_n^{(1)}(t), u_n^{(2)}(t)$ from $t=25$ to $t=225$. Again (Fig. 3) the solutions deviate significantly, although the growth rate of the difference is smaller than in the previous case. Furthermore, imposing a small random perturbation at each time step (for $t \geq 25$), we find a more rapid growth of the deviation to an $O(1)$ value.

For defocusing NLS all the difficulties encountered in the focusing case disappear. The power spectrum of a

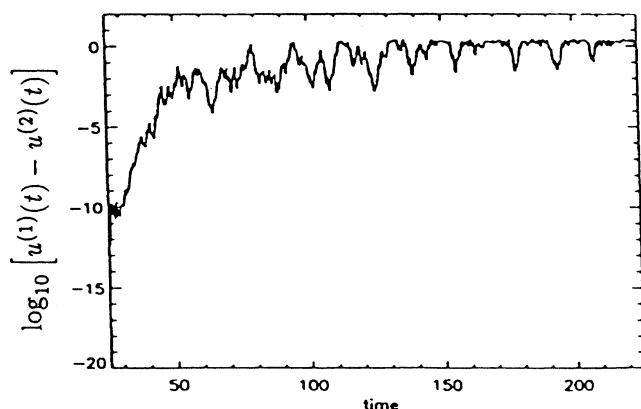


FIG. 3. The growth in the difference of solutions for IDNLS for the nonlinear regime.

typical solution [compare with Fig. 1(b)] is plotted in Fig. 4 where we take $g(x, \epsilon), \epsilon = 10^{-1}$. We observe no growth of asymmetry and both algorithms IDNLS and FSS show no growth in the difference between solutions $u_n^{(1)}$ and $u_n^{(2)}$. Recall that the periodic defocusing NLS does not have homoclinic structures. Small errors do not grow rapidly and IDNLS and FSS are accurate predictors of the long time behavior of the solution.

Since we are studying initial data which are small deviations from a constant, we are able to calculate the periodic or antiperiodic eigenvalues of 2-3 via perturbation analysis (see e.g., [8]). For the initial data $g(x, \epsilon) = a(1 + \epsilon \cos 6\mu x)$ with ϵ small, at leading order there are eight complex eigenvalues which are double points (i.e., eigenvalues of multiplicity 2). Each of these double points corresponds to an unstable mode. We find that under perturbation the double point corresponding to the perturbation 6μ is split by $O(\epsilon)$. The other complex double points, while translating by $O(\epsilon^2)$ nevertheless have a splitting distance which is smaller than any power of ϵ . The splitting distance of the remaining complex eigenvalues is beyond all orders in ϵ . Consequently, we are "exponentially close" to the homoclinic manifolds, and small deviations on the order of roundoff can lead to homoclinic crossings and the observed chaos. We have extended our perturbation analysis to predict how modifications in the initial values of earlier numerical simulations [3] could lead to homoclinic crossings under tiny perturbations such as roundoff. We believe that this mechanism can also explain similar difficulties observed, but not understood, in other Hamiltonian equations [9].

The extreme proximity of these data values to the unperturbed homoclinic manifolds prevents us from numerically calculating the "true" solution after moderate time. The calculations are influenced by minuscule errors; computationally the NLS equation is "effectively chaotic" in this range of parameter space despite it being "integrable." Since NLS is so special, we expect an underlying structure to the temporal disorder which may be determined by appropriate statistical studies. Numerical

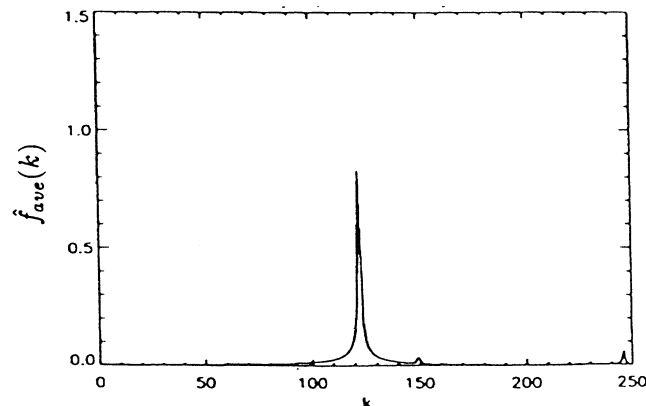


FIG. 4. The power spectrum for defocusing IDNLS with $g(x, \epsilon = 10^{-1})$.

simulations which test the stability of small odd perturbations, rearrangements of terms, complex nonlinear states, such as those mentioned in this Letter, can demonstrate the existence of serious underlying numerical instabilities even when known constants of the motion are seemingly well preserved. A more complete account of the work described here will be published in a future paper.

We thank E. Overman for the use of his spectral solver package and R. McLachlan for useful discussions. This work was partially supported by the Air Force Office of Scientific Research under Grant No. AFOSR-90-0039, the NSF Grant No. DMS-9024528, and the Office of Naval Research Grants No. N00014-91-J-4037 and No. N00014-92-J-1274.

*Present and permanent address: University of the Orange Free State, Bloemfontein 9300, South Africa.

- [1] M. J. Ablowitz and P. A. Clarkson, *Solitons, Nonlinear Evolution Equations and Inverse Scattering* (Cambridge Univ. Press, Cambridge, 1991); A. R. Its and V. P. Kotlanov, Dokl. Akad. Nauk. Ukain. SSR Ser. A, **11**, 965 (1976).
- [2] B. M. Herbst and M. J. Ablowitz, Phys. Rev. Lett. **62**, 2065 (1989); D. W. McLaughlin and C. M. Schober, Physica (Amsterdam) **57D**, 447 (1992); G. Forest, C. Goedde, and A. Sinha, Phys. Rev. Lett. **68**, 2722 (1992).
- [3] H. C. Yuen and W. Fergusen, Jr., Phys. Fluids **21**, 1275 (1978); H. C. Yuen and B. M. Lake, Phys. Fluids **18**, 956 (1975).
- [4] M. J. Ablowitz and J. F. Ladik, J. Math. Phys. **17**, 1011 (1976).
- [5] J. A. C. Weideman and B. M. Herbst, SIAM. J. Numeric. Anal. **23**, 485 (1986).
- [6] P. J. Channel and C. Scovel, Nonlinearity **3**, 231 (1990).
- [7] Y. C. Ma and M. J. Ablowitz, Stud. Appl. Math. **65**, 113 (1982).
- [8] M. J. Ablowitz and B. M. Herbst, in *Proceedings of the CRM, Hamiltonian Systems, Transform Groups and Spectral Transform Methods* (University of Montreal Press, Montreal, 1989).
- [9] B. Fornberg and G. Whitham, Philos. Trans. R. Soc. **289**, 373 (1978).